DINAME 2023 - Proceedings of the XIX International Symposium on Dynamic Problems of Mechanics,
A.S. De Paula, A.T. Fabro and M.R. Machado (Editors), ABCM.
Pirenópolis, Go, Brazil, February 26th to March 3rd, 2023

Low-order Hypersonic Vehicle Trajectory Simulator

Robert R. A. Oliveira[1], Alexandre N. Barbosa[2], Angelo Passaro[2], and Roberto G. A. da Silva[1]

[1] Instituto Tecnológico de Aeronáutica (ITA), Praça Marechal Eduardo Gomes, 50 - Vila das Acácias, CEP 12228-900, São José dos Campos - SP, Brazil

[2] Instituto de Estudos Avançados (IEAv), Trevo Coronel Aviador José Alberto Albano do Amarante, 1 - Putim, CEP 12228-001, São José dos Campos - SP, Brazil

Abstract: The development of accurate simulators depends on experimental data and high-fidelity simulators used as a benchmark. The methodology for the development of new simulators consists of successive refinements starting with low-order models. Low-order models allow the overall parameters evaluation of a project in its early stages. This article introduces a low-order simulator called Low-order Hypersonic Vehicle Trajectory Simulator (LHVTS). Its validation consists of comparing the results with the program ROSI, a computational tool validated for decades with experimental flight data. LHVTS is applied in a case study of a hypothetical hypersonic vehicle that must be accelerated by a Brazilian VSB-30 rocket until reaching Mach 6.8 on atmospheric re-entry at a geometry altitude of 30 km. It is concluded that the hypothetical hypersonic vehicle and its service module must weigh less than 400 kg to achieve these flight conditions. Results like this illustrate the usefulness of low-order models in evaluating overall design parameters to determine some of the key requirements of a hypersonic vehicle. In addition, the application of the LHVTS demonstrated a low computational cost for determining the results of general design parameters of models with precision similar to the results obtained through higher order models, such as ROSI, for example, which is one of the advantages of using low-order models.

Keywords: Trajectory simulator, low-order models, hypersonic vehicle, VSB-30.

INTRODUCTION

A hypersonic vehicle simulator is a computer program. Based on a set of mathematical models, the simulator calculates position, velocity, and other object path parameters in one or more frames of reference. The simulator uses the model of a particle, or a body, to represent the object. In the simulator, differential equations govern the movement of the object. The result depends on the initial conditions, subject to the continuous actions of forces and moments. The simulator calculates the object path in phases characterized by abrupt changes in the object's properties. Depending on the intended fidelity of the simulator, a particle, a rigid or flexible body can represent a hypersonic vehicle. The movement starts on a launch pad and goes forward by propelled and ballistic phases, affected by Earth's gravity and atmosphere, eventually interspersed with abrupt changes in the object's mass due to the separation of its parts.

There is a wide variety of trajectory simulators. However, few simulators have their mathematical models validated by experimental data over decades, as the program ROSI (Rocket Simulator) is the case with, written in Fortran. For this reason, ROSI can be used as a benchmark to validate other simulators. For example, as it is a high-fidelity program, ROSI is used by Barbosa and Guimarães (2012) in their MDO-SONDA tool, where it calculates the trajectory for optimizing suborbital vehicles. A hypersonic vehicle is an object that moves at a speed greater than Mach 5, using a scramjet engine, which operates exclusively in this speed range, requiring, for this reason, a conventional rocket to be accelerated until reaching the endoatmospheric flight conditions for its activation (Fortescue et al., 2011, p. 198). Different from conventional rockets, the scramjet engine sucks the oxidant from the atmospheric air to carry out a supersonic combustion. A conventional rocket can reach hypersonic speeds, but it must carry the oxidant in its tanks. The two technologies' combination is a way to take advantage of their features and produce an artifact that performs better than these technologies take separately.

The 14-X, a project conducted by the Institute for Advanced Studies (IEAv), is an example of a hypersonic vehicle. Its first launch took place in 2021. The VSB-30 is the Brazilian conventional rocket chosen to accelerate the 14-X until it reaches its activation conditions. Palmerio et al. (2003) introduces the development of the VSB-30 in partnership with the German Space Agency (DLR). The VSB-30 originates from technologies previously developed by the Institute of Aeronautics and Space (IAE), combined with a payload module developed by the DLR. According to de Rêgo et al. (2019), since 2015, the VSB-30 has been used for hypersonic flight tests. Garcia et al. (2011) provide details on the performance of the VSB-30 by analyzing ten of its launches. The VSB-30 is composed of two stages. Both stages use solid propellant motors, the S31, and the S30, respectively.

The development of accurate simulators depends on experimental data to validate the mathematical models used in them. Generally, the validation considers the comparisons with scientific articles, more advanced computational tools, and experimental data. An approach to advance in simulators is to drive their development through successive refinements and tests. The development begins with low-order models, testing them before moving on to higher-order ones. This is

a sequential refinement technique, one of the main concepts of structured programming, which reduces the occurrence of errors during software development (Farrer, 1999, p. 175). Low-order models require less data than higher-order models, can be as accurate as higher-order models in calculating overall design parameters, and can eventually add new functionalities. Therefore, it is interesting to start the development with low-order models.

This article presents a computational program for trajectory calculation in two-dimensional space called Low-order Hypersonic Vehicle Trajectory Simulator (LHVTS), written in Python, within the scope of the National Developments in Aspired Hypersonic Propulsion, with a focus on Access to Space and Defense (PROCAD-DEFESA), for academic use. This tool has only two degrees of freedom (2-DoF), so it is a low-order simulator in this sense. The model used in LHVTS allows simulating turning maneuvers. In the ascending flight, aerodynamically stable rockets fly in the atmosphere with an angle of attack around zero due to their fins. When the lift force increases due to the opening of an angle of attack, the rocket restores its stability, generating an aerodynamic moment that reduces the angle of attack again. The turning is only due to gravity, being called gravity turn (Cornelisse et al., 1979, p. 255). Applying a turning maneuver in the descending phase of the trajectory due to the resultant between gravity and lift force, it is possible to predict the general behavior of a hypersonic vehicle in atmospheric re-entry.

Here is a contextualization of relevant aspects of trajectory simulators and hypersonic vehicles. The following sections describe the mathematical model that covers the motion equations described for the dynamic models inserted in LHVTS. Then, in LHVTS' features, it is presented on the working process and the parameters calculated by the simulator. Finally, before concluding, the results obtained with validation and re-entry simulation of a hypersonic vehicle are shown and discussed.

MATHEMATICAL MODEL

Unlike ROSI, LHVTS only works with a particle model in a two-dimensional space, which cannot predict the aerodynamic stability of the VSB-30. However, the turning maneuver formulation is inserted in LHVTS, artificially reproducing the behavior of an aerodynamically stable vehicle on its propelled flight (Cornelisse et al., 1979, p. 255). In this way, it is possible to calculate the trajectory profile of a hypersonic vehicle in the ascending and re-entry phase considering only 2-DoF. The fundamentals of the turning maneuver are in the rotational mechanics of a particle. When the turning maneuver is on, the radial velocity of the particle is not affected by the radial and tangential acceleration. Only the tangential velocity is affected by the acceleration components. Its magnitude is affected by the tangential acceleration. And its direction is affected by the radial acceleration. The turning maneuver due to gravity is called gravity turn, which is performed to reduce the aerodynamic forces found in the densest layers of the atmosphere by the vehicle on the ascending flight, where the angle of attack tends to zero. The equations of motion, described below, consider the generic formulation of the turning maneuver in Eq. (3), which includes the gravity, drag and lift forces.

$$\frac{dv_{x'}}{dt} = \frac{E}{m} + g_{x'} + \frac{D_{x'}}{m} + \frac{L_{x'}}{m} \tag{1}$$

$$\frac{dv_{y'}}{dt} = 0 \tag{2}$$

$$\frac{d\theta}{dt} = -\frac{g_{y'} + \frac{D_{y'}}{m} + \frac{L_{y'}}{m}}{v_{x'}} \tag{3}$$

$$\begin{bmatrix} \frac{dv_x}{dt} \\ \frac{dv_y}{dt} \end{bmatrix} = \begin{bmatrix} \cos\theta & \sin\theta \\ \sin\theta & -\cos\theta \end{bmatrix} \begin{bmatrix} \frac{dv_{x'}}{dt} \\ \frac{dv_{y'}}{dt} \end{bmatrix} \tag{4}$$

$$\frac{dx}{dt} = v_x \tag{5}$$

$$\frac{dy}{dt} = v_y \tag{6}$$

In the above equations, $v_{x'}$ and $v_{y'}$ are the velocity components in the vehicle's reference frame; θ is the vehicle's axis elevation angle; E is the thrust force; m is the mass of the vehicle; $g_{x'}$ and $g_{y'}$ are the components of the gravitational acceleration in the vehicle's reference frame; $D_{x'}$ and $D_{y'}$ are the components of the drag force in the vehicle's reference frame; $L_{x'}$ and $L_{y'}$ are the components of the lift force in the vehicle's reference frame; v_x and v_y are the velocity components in the inertial reference frame; and x and y are the position components in the inertial reference frame. The equations of motion that consider the turning maneuver are one of the models present in LHVTS. Two other dynamic models are present in order to calculate the trajectory profile during the flight on the ramp and without taking into account the turning maneuver. During the flight on the ramp, the vehicle is supported on it and, therefore, moves only along its longitudinal axis. As the ramp is fixed at a point on the Earth, the vehicle rotates along the ramp with a constant velocity equal to the rotation velocity of the Earth, Eq. (7). The equations of motion Eq. (1), Eq. (2), Eq. (4), Eq. (5) and Eq. (6), together with the equation described below, describe the vehicle movement on the ramp (Fig. 1).

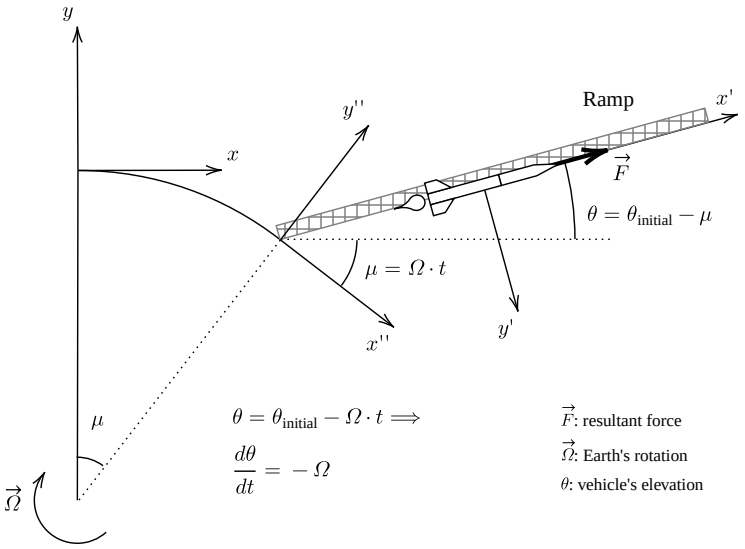

Figure 1: Vehicle movement on the ramp.

$$\frac{d\theta}{dt} = -\Omega \tag{7}$$

In Eq. (7), Ω is the angular velocity of Earth's rotation. When turning maneuvers are not considered, the vehicle flies freely in space and can be represented by a model based on the Tsiolkovsky's rocket equation. The equations of motion Eq. (1), Eq. (4), Eq. (5) and Eq. (6), together with the Eq. (8) and Eq. (9), consider the free flight.

$$\frac{dv_{y'}}{dt} = g_{y'} + \frac{D_{y'}}{m} + \frac{L_{y'}}{m} \tag{8}$$

$$\frac{d\theta}{dt} = -q \tag{9}$$

In the Eq. (9), q is the constant pitch rate at which the vehicle can be subjected. It can represent a residual angular velocity arising from a maneuver performed before, from the gravitational rotation, for example, or related to an input data inserted according to the needs of the simulated case in order to tilt the vehicle frame. In this case, it does not mean that there is an additional degree of freedom in rotation, as the rotation is not caused by the dynamics of a rigid body. The aerodynamic forces are calculated as a function of the vehicle's relative velocity to the stationary atmosphere. The equations of motion describe the trajectory in free space with a gravitational field varying along the curvature of the Earth, considering the thrust force and the variable mass along the trajectory, the aerodynamic drag and lift forces, the Earth's rotation, and the atmospheric model (Fig. 2).

LHVTS' FEATURES

The simulator integrates the equations of motion. The integration occurs in phases starting with the vehicle on the ramp, followed by propelled and ballistic flights in ascending and descending trajectory, and ending with the vehicle's re-entry into the atmosphere. The trajectory calculation in phases come from abrupt changes in the vehicle's properties as the separation of stages, the ignition and interruption of the engines, and the changes in the flight dynamics. An example is the trajectory change of the vehicle from the movement on the ramp to the turning maneuver. Each change in flight dynamics is described by a mathematical model with specific equations of motion as shown in the previous section.

There are different ways to model the turning maneuver. For example, if the equations are written in the vehicle's frame system, as in the LHVTS, the component of the velocity in the direction of the thrust vector is the tangential velocity of the vehicle. The velocity normal to that direction is the radial velocity of the vehicle. When performing an integration step, the magnitude of the tangential velocity and the rotation angle of this velocity are updated. However, before performing the next integration step, it is necessary to apply the rotation to the tangential velocity. After rotating, there are two components based on the previous tangential velocity, a component in the thrust direction and a normal one that is added to the previous radial velocity (Fig. 3). Therefore, the implementation of the turning maneuver consists of two operations. First, by updating the magnitude of the tangential velocity and its angle of rotation, the elevation angle θ,

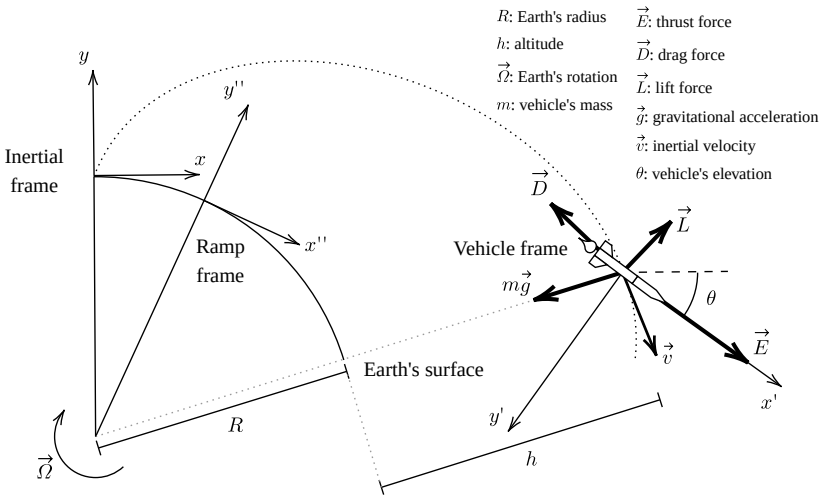

Figure 2: Free body diagram.

performing an integration step. Second, after executing the integration step, by applying the rotation angle to update the velocity components in the vehicle's frame system.

LHVTS uses the 4th Order Runge-Kutta method to solve the system of differential equations of the vehicle motion. After an integration step, the Eq. (10) calculates the inertial velocity once the Eq. (3) updates the vehicle's axis elevation.

$$\begin{bmatrix} v_{x_{i+1}} \\ v_{y_{i+1}} \end{bmatrix} = \begin{bmatrix} \cos\theta_i & \sin\theta_i \\ \sin\theta_i & -\cos\theta_i \end{bmatrix} \begin{bmatrix} v_{x'_{i+1}} \cos\Delta\theta \\ v_{y'_{i+1}} + v_{x'_{i+1}} \sin\Delta\theta \end{bmatrix} \tag{10}$$

In Eq. (10), $v_{x_{i+1}}$ and $v_{y_{i+1}}$ are the velocity components in the inertial reference frame after the i-th integration step; θ_i is the vehicle's axis elevation at the i-th integration step; $v_{x'_{i+1}}$ and $v_{y'_{i+1}}$ are the velocity components in the vehicle's reference frame after the i-th integration step; and $\Delta\theta$ is the increment of the vehicle's axis elevation after the i-th integration step (Fig. 3).

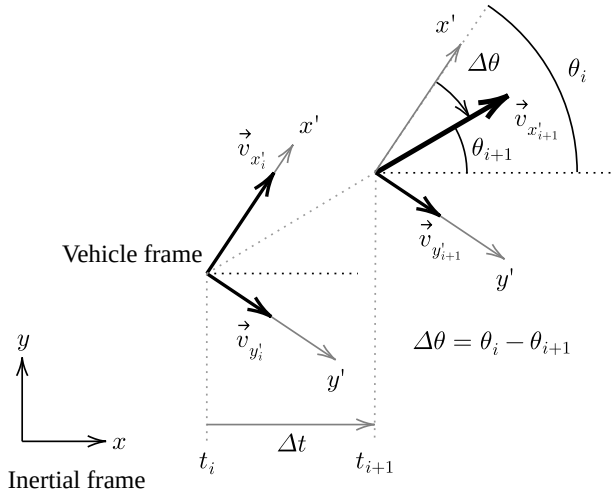

Figure 3: Velocity correction after a step integration.

Different trajectories can be analyzed by inserting more mathematical models according to flight requirements. The complete trajectory is made up of the flight phases. Therefore, it is possible to obtain parameters such as velocity, position, dynamic pressure, Mach number, elevation, trajectory, and attack angles, all as a function of time, among other performance features. In addition to the LHVTS's mathematical models, it is also possible to incorporate models from different areas of knowledge. Routines can be performed before, during, and after the integration of the equations of motion. For example, structural routines can provide input data for trajectory calculation. Control systems and flexible

body models act in a way that is coupled to flight dynamics. Thermal routines are performed on the resulting flight parameters.

Table 1 shows the features comparison with ROSI. In order to compare the results with the ROSI, some of its mathematical models are adopted. The world geodetic system used is the WGS 84, and the calculation of the two-dimensional trajectory is related to the equator plane. The standard model of the atmosphere is from 1962. In the initial conditions, a launch point is adopted at sea level, given as the origin of the coordinate system.

Table 1: Comparison of the main differences between ROSI and LHVTS.

	LHVTS	ROSI
Body model	Particle	Rigid body/Particle
Space	Two-dimensional	Three-dimensional
Degrees of freedom	2-DoF	6-DoF/3-DoF
Turning maneuver	In pitch	Not available
Re-entry	Drag and lift	Drag

The LHVTS calculates the trajectory with just 2-DoF, approaching the vehicle by a particle, considering its translations in two-dimensional space. However, the LHVTS is capable to execute a turning maneuver, allowing to simulate an aerodynamically stable vehicle and making it possible to maneuver the vehicle in the re-entry considering the resultant between the force of gravity and lift. Thus, it is noted that the LHVTS does not need a rotational degree of freedom to simulate an aerodynamically stable vehicle in two-dimensional space, making it computationally faster. On the other hand, ROSI does not have the turning maneuver among its features and calculates the trajectory, in the ascending phase, considering the translation and rotation of the vehicle in 6-DoF with rigid body model. The program was developed to simulate an aerodynamically stable vehicle in three-dimensional space. In the descending phase, ROSI calculates the trajectory considering only the vehicle's translation in 3-DoF with particle model, including only the drag force. Generally, the stability condition does not occur in the descending phase of the trajectory. The following section demonstrates the application of LHVTS versus ROSI in assessing the capability of a VSB-30 to accelerate a hypothetical hypersonic vehicle to achieve its endoatmospheric flight conditions.

RESULTS AND DISCUSSION

The validation methodology consists of LHVTS and ROSI comparison, referring to the flight of the VSB-30 V07 in the Maracati II operation, performed in 2010 (Garcia et al., 2011). Among the available input parameters, both simulators use the thrust curves of the rocket engines, the rocket mass curve, and the drag coefficients of that specific flight. In addition, for demonstration purposes, it is assumed that the hypothetical hypersonic vehicle's aerodynamic coefficients are that one of the payload carried by the VSB-30 V07. In a complementary way, the mass curves are determined since their variation occurs due to the propellant consumption. Static firing tests are essential to describe the behavior of engines. However, the aerodynamic coefficients are established through mathematical models. As the VSB-30 has a geometry with axial symmetry, these models can accurately determine the aerodynamic coefficients. The Missile Datcom software is used to compute the aerodynamic parameters in a project quickly and economically (Rosema et al., 2011). Its mathematical models are exhaustively compared to wind tunnel tests for validation. With respect to the hypersonic vehicle, the generic operating conditions, described in Toro et al. (2018), are assumed. The study focused on designing a scramjet engine configuration based on a full-scale generic geometry. Given this, the vehicle must be accelerated to Mach 6.8 at the geometric altitude of 30 km before it can be activated.

Figure 4 shows the parameters obtained with the validation process of the LHVTS through its comparison with the ROSI. According to the trajectory profile in Fig. 4a, the VSB-30 reaches an apogee of 252.9 km and travels a distance of 153.6 km. It is also noted that total velocities above 2000 m/s are reached in atmospheric flight in the ascending and re-entry phases (Fig. 4b). Even the LHVTS having 2-DoF during the entire trajectory, results were obtained similar to those calculated by the ROSI, which considers 6-DoF during the ascending atmospheric flight phase and 3-DoF for the rest of the trajectory. In the ascending phase, there are two dynamic pressure peaks, but the vehicle suffers greater stress during the re-entry flight, as expected, with a maximum dynamic pressure of 862.8 kPa (Fig. 4c). It is important to be aware of the dynamic pressure on re-entry so that the hypersonic vehicle can be designed to support it, avoiding possible damage to its structure or deviations in flight dynamics. Analogous to the total velocity, there are Mach number peaks in the ascending and re-entry phases of atmospheric flight greater than 6 (Fig. 4d). These intervals present the possibility of activating the hypersonic vehicle. Therefore, it is needed to analyze them together with the altitude to verify if the operational conditions are reached.

After validation, a simulation was performed using LHVTS in order to analyze the activation of the scramjet engine present in the hypersonic vehicle. In addition to the aforementioned input parameters, lift coefficients were also used as input parameters. As the turning maneuver used for reentry of the hypothetical hypersonic vehicle starts from the instant

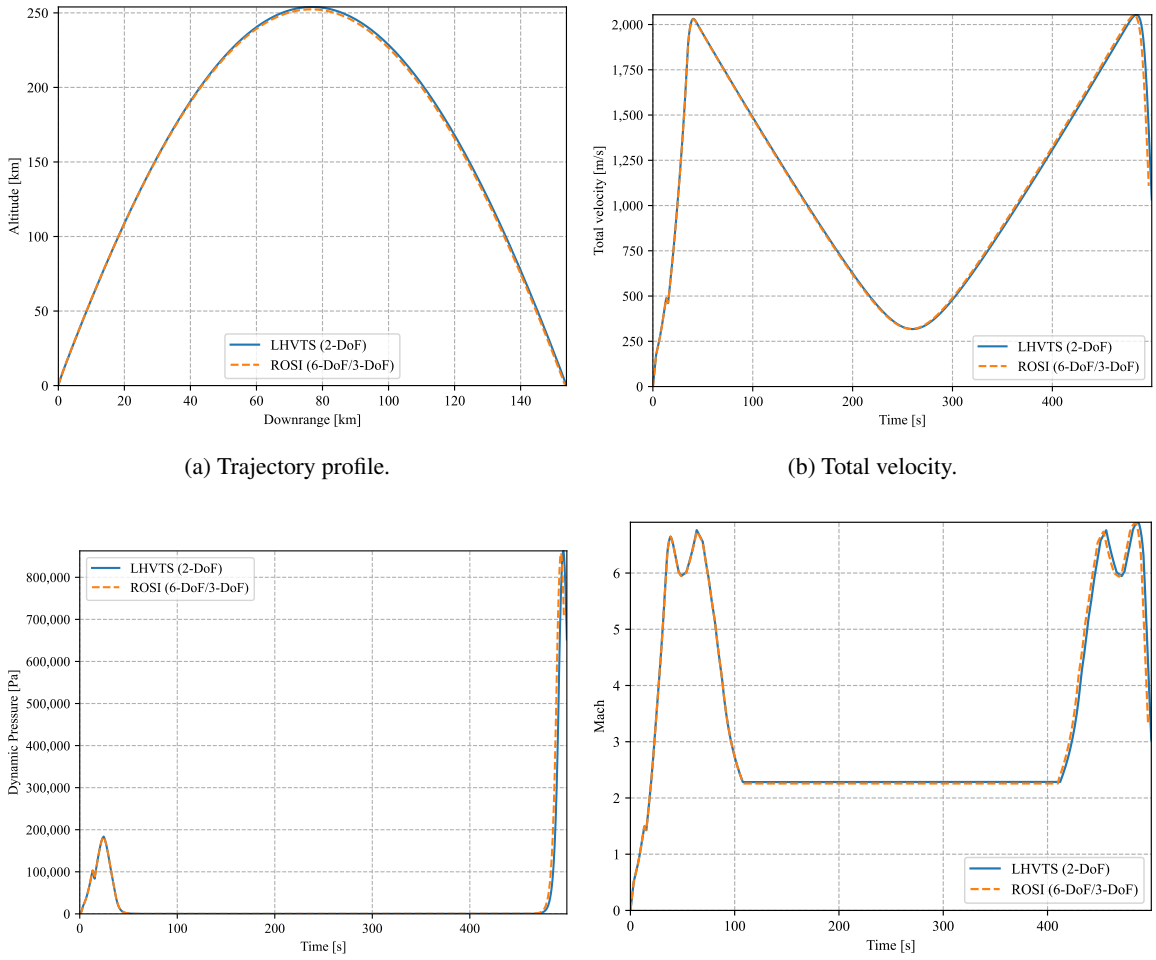

(a) Trajectory profile.

(b) Total velocity.

(c) Dynamic pressure.

(d) Mach number.

Figure 4: LHVTS's validation.

of 460 seconds, when the vehicle reaches the densest layers of the atmosphere, the main differences between the results are seen after this instant. The parameters obtained with the simulation of the hypothetical hypersonic vehicle re-entry using LHVTS are compared to the tracings by ROSI during the validation in Fig. 5. The VSB-30 maintained its apogee of 252.9 km and, as shown in Fig. 5a, the distance traveled increased to 170.4 km, due to the turning maneuver performed on the hypersonic vehicle's re-entry. The total velocity, in the turning maneuver, remained identical to that simulated in the validation, having only an extension of the curve in time, since the vehicle had its trajectory slightly extended (Fig. 5b). There were no changes in dynamic pressure in the ascending phase, as expected. However, there was a reduction in the value of the maximum dynamic pressure on vehicle re-entry, reducing to the value of 745.59 kPa (Fig. 5d). This result suggests that the turning maneuver can be used to generate less aggressive conditions for the hypersonic vehicle's flight, and to reduce its project cost. The Mach number behaved similarly to total velocity, remaining the same as the validation simulation with an extension of the curve due to the increase in the distance traveled (Fig. 5c).

Figure 6 presents the behavior of the angle of attack during the ascending phase of atmospheric flight and in the turning maneuver used for reentry of the hypersonic vehicle. In ascending flight, there are differences between the curves reproduced by the simulators due to the difference between their dynamic and body models, but the gravity turn maneuver caused the angle of attack calculated by LHVTS to tend to zero as expected (Fig. 6a). To perform the re-entry maneuver, it was necessary to reduce the angle of attack to values below 8 degrees (Fig. 6b). Note that, from that moment on, the angle of attack decreases more gradually, tending to zero. Thus, the lift can act on the vehicle and provide its glide during the execution of the maneuver and activation of the scramjet engine.

Figure 7 shows the VSB-30 capability to accelerate a hypothetical hypersonic vehicle weighting less than 400 kg. Both simulators calculate the maximum Mach, of 6.9, at the altitude of 21.7 km on the atmospheric re-entry (Fig. 7b). According to Fig. 7a, the VSB-30 does not reach the maximum value of Mach in the ascending flight. The simulators do not match in the descending flight from the altitude of 12 km due to the lift effect took into account in LHVTS's flight dynamic model. The deviation is caused by an angle of attack less than 8 degrees. Since the general flight condition for the hypothetical hypersonic vehicle is fulfilled by the VSB-30, in the range from 29.9 km to the geometric altitude of 17

km, providing a Mach greater than 6.8, the lift effect caused by small angles of attack do not have influence in the scramjet activation.

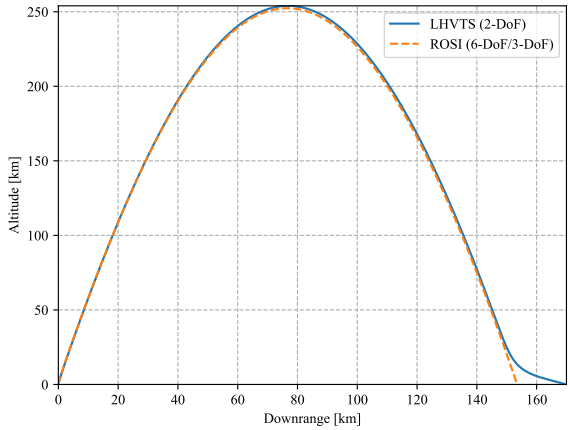

(a) Trajectory profile.

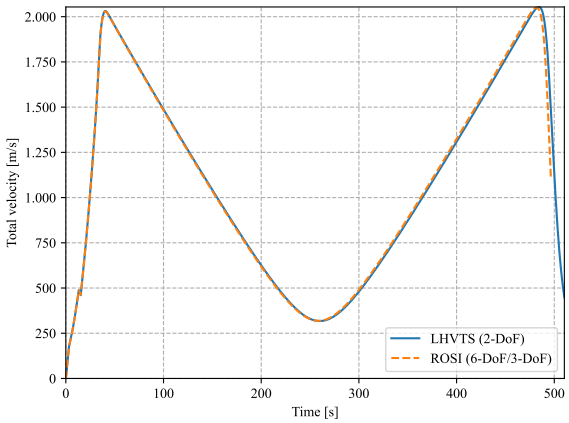

(b) Total velocity.

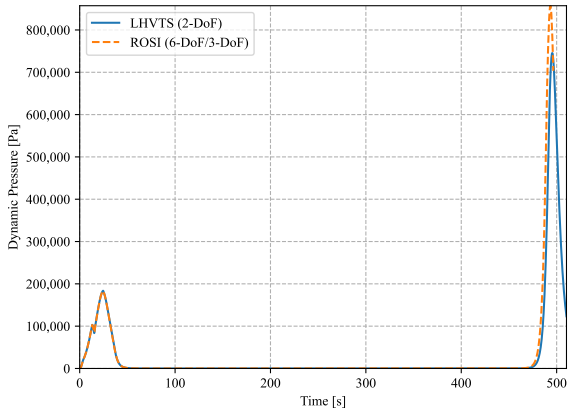

(c) Dynamic pressure.

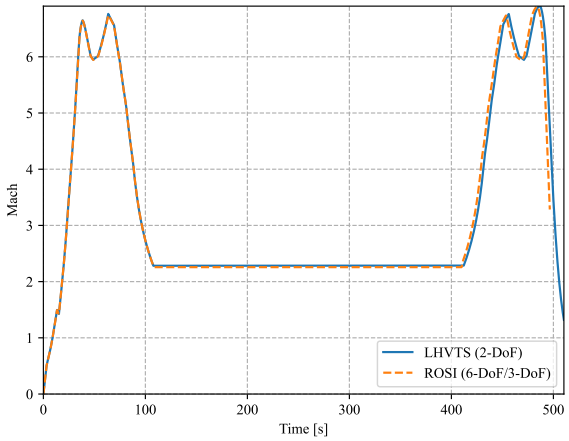

(d) Mach number.

Figure 5: Hypersonic vehicle re-entry simulation.

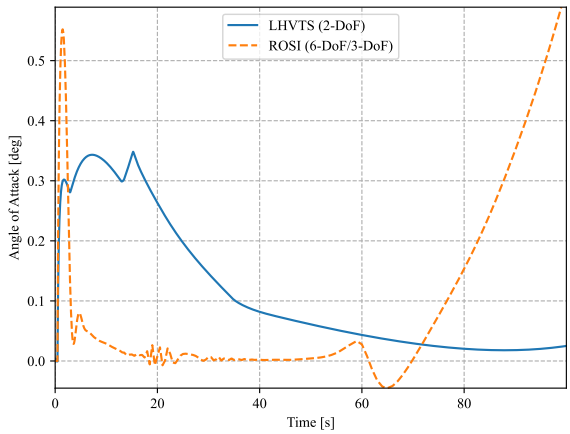

(a) Ascending flight.

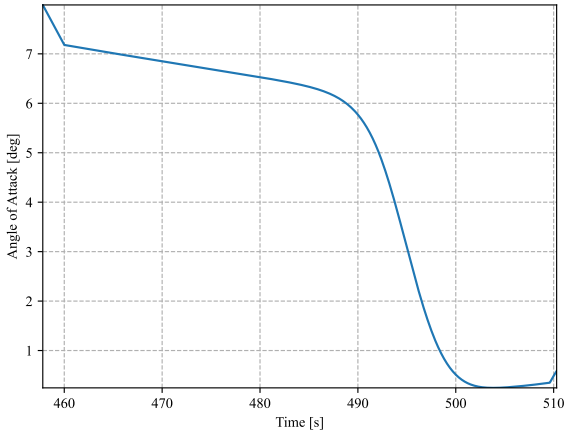

(b) Reentry after turning maneuver.

Figure 6: Angle of Attack.

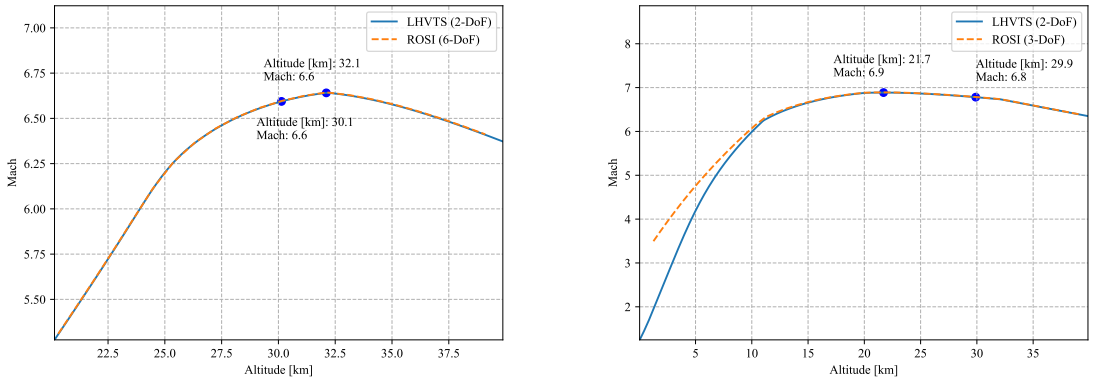

(a) Ascending flight.

(b) Re-entry.

Figure 7: VSB-30's performance.

Since the model and input data are very accurate, the results of the hypothetical hypersonic vehicle can be used to establish the trends for a true project using the VSB-30 acceleration capability. For example, it can be inferred, if no optimization is considered, that the weight of a hypersonic vehicle and its service module cannot exceed 400 kg if it has to reach Mach 6.8 on atmospheric re-entry at an altitude of 30 km. This case illustrates the importance of low-order simulators like LHVTS. LHVTS requires less input data than ROSI, gives a very accurate result like ROSI, and predicts the lift effect on atmospheric re-entry beyond ROSI.

In view of the relevance of the application of the LHVTS, it is intended to develop further studies taking advantage of the features of this simulator in the future. In order to evaluate the optimization of stages, or even of the hypersonic vehicle, it is planned to couple the LHVTS to the LEV optimization framework (LOF), presented by Saba (2017), and with an optimization method based on Lagrange's multipliers, presented by Oliveira and Barbosa (2021). Furthermore, it is intend to develop dynamic models considering a planar rigid body model to deal with the control system of the hypersonic vehicle in the re-entry phase. Finally, it is also intend to model the equations of motion to deal with aeroelastic phenomena in the trajectory calculation using a flexible body model. The experience gained with this simulator allows the development and testing of more complex mathematical models to calculate a larger set of path parameters for hypersonic vehicles, in three-dimensional space, considering 6-DoF in the ascending and descending phases of flight.

CONCLUSION

The objective of this article was achieved by demonstrating the usefulness of low-order models in the determination of general parameters of hypersonic vehicles. A mathematical model was presented including the turning maneuver in the equations of motion, which allows evaluating the influence of lift on the vehicle's performance in the atmospheric re-entry phase. Thus, evidencing the implementation potential for new features in low-order models. It was concluded that, for the hypothetical case analyzed, the lift does not affect the moment of flight in which the accelerator rocket reaches the conditions of activation of the scramjet engine. This example illustrates the application of low-order models in determining eventual design requirements for hypersonic vehicles. These models can accurately reproduce project results at low computational cost, compared to higher order models. This also offers opportunities to add more routines from other disciplines, such as control and flexible body, to coupling optimization frameworks, and to introduce more complex mathematical models to calculate trajectories with 6-DoF.

ACKNOWLEDGMENTS

This study was financed by the Coordenação de Aperfeiçoamento de Pessoal de Nível Superior - Brasil (CAPES) - Finance Code 001 and was carried out with the support of the Academic Cooperation Program in National Defense (PROCAD-DEFESA), grant 88881.387753/2019-01.

REFERENCES

Barbosa, A.N. and Guimarães, L.N.F., 2012, "Multidisciplinary design optimization of sounding rocket fins shape using a tool called MDO-SONDA". Journal of Aerospace Technology and Management, Vol.4, pp. 431–442.

Cornelisse, J.W., Schöyer, H.F.R. and Wakker, K.F., 1979, "Rocket Propulsion and Spaceflight Dynamics". Pitman.

Farrer, H., 1999, "Programação estruturada de computadores: algoritmos estruturados". LTC Editora.

Fortescue, P., Swinerd, G. and Stark, J., 2011, "Spacecraft systems engineering". John Wiley & Sons.

Garcia, A., Yamanaka, S.S.C., Barbosa, A.N., Bizarria, F.C.P., Jung, W. and Scheuerpflug, F., 2011, "VSB-30 sounding rocket: history of flight performance". Journal of Aerospace Technology and Management, Vol.3, pp. 325–330.

Oliveira, E. J. D. and Barbosa, A. N., 2021, "Micro Launcher Optimum Design Using the Solid Rocket Motor S-50". In Proceedings of the 72nd International Astronautical Congress (IAC), 28th International Academy of Astronautics (IAA), Dubai, United Arab Emirates, October 25-29, 2021. International Astronautical Federation (IAF).

Palmerio, A.F., Peres da Silva, J.P.C., Turner, P. and Jung, W., 2003, "The Development of the VSB-30 Sounding Rocket Vehicle". In Proceedings of the 16th ESA Symposium on European Rocket and Baloon Programmes and Related Research, Vol.530, Sankt Gallen, Switzerland, pp. 137-140.

Rêgo, I.S., Passaro, A., Carinhana Junior, D., Sala Minucci, M.A. and de Oliviera, É.J., 2019, "Brazilian Suborbital Rockets for Hypersonic Flight Testing: A Review and a Market Perspective". In Proceedings of the 70th International Astronautical Congress, Washingtong DC, United States.

Rosema, C., Doyle, J., Auman, L., Underwood, M. and Blake, W.B., 2011, "MISSILE DATCOM user's manual-2011 revision". Army Aviation and Missile Research Development ENG CTR Redstone Arsenal AL System Simulation and Development Directorate.

Saba, W.B., 2017, "Optimization framework based on metaheuristics (in portuguese)". Master's thesis, Graduate Program in Space Sciences and Technologies, Instituto Tecnológico de Aeronáutica, São José dos Campos, Brasil.

Toro, P., Carneiro, R., Araújo, J. W. S., Marinho, G. S., Borba, G. L., Martos, J. F. A. and Rêgo, I. S., 2018, "Design of the generic scramjet combustion chamber". In Proceedings of the 17th Brazilian Congress of Thermal Sciences and Engineering, Águas de Lindóia, SP, Brazil.

RESPONSIBILITY NOTICE

The authors are the only responsible for the printed material included in this paper.